Available online at www.sciencedirect.com

SciVerse ScienceDirect

Ceramics International 39 (2013) 2709–2714

CERAMICS INTERNATIONAL

www.elsevier.com/locate/ceramint

Fluorescence improvement of $Ba_{1.3}Ca_{0.7}SiO_4$:Eu^{2+},Mn^{2+} phosphors via Dy^{3+} addition and their color-tunable properties

Zhi Huang, Yong-Jie Chen*, Lin Chen, Ying Xie, Lin-Jiu Xiao, Ying Yang

Key Laboratory of Rare Earth Chemistry and Application of Liaoning Province, Shenyang University of Chemical Technology, Shenyang, China

Received 10 June 2012; received in revised form 1 September 2012; accepted 13 September 2012
Available online 19 September 2012

Abstract

A series of novel single-phase white phosphors $Ba_{1.3}Ca_{0.69-x-y}SiO_4$:$0.01Eu^{2+}$,$xMn^{2+}$, yDy^{3+} were synthesized by the solid-state method. The excitation spectra of these phosphors exhibit a broad band in the range of 260–410 nm, which can meet the application requirements for near-UV LED chips (excited at 350–410 nm). The emission spectra consist of two broad bands positioned around 455 nm and 596 nm, which are assigned to 5d→4f transition of Eu^{2+}, and $^4T_1 \rightarrow {}^6A_1$ transition of Mn^{2+}, respectively. The luminescence intensity of phosphors enhances obviously by doping Dy^{3+} ions, and the intensity of two bands reaches an optimum when Dy^{3+} amounts to 2 mol%. In addition, thermoluminescence investigation of phosphor was conducted, getting two shallow trap defects with activation energy of 0.43 eV and 0.45 eV, which demonstrates the energy transfer mechanism of Dy–Eu through the process of hole and electron traps. By precisely tuning the Mn^{2+} content, an optimized white light with color rendering index (CRI) of $R_a=84.3\%$, correlated color temperature (CCT) of $T_c=8416$ K and CIE chromaticity coordinates of (0.2941, 0.2937) is generated. The phosphor could be a potential white phosphors for near-UV light emitting diodes.

Keywords: D. Silicate; D. Phosphor; D. $Ba_{1.3}Ca_{0.7}SiO_4$:Eu^{2+},Mn^{2+},Dy^{3+}; E. Light-emitting-diode

1. Introduction

White light-emitting diode (W-LED) is considered as the most promising light source, due to the merits of a long life span, compact size, high brightness, low energy consumption, and environmental friendliness, which has aroused wide public concern during the past 30 years [1–6]. Currently, white light-emitting diode produced by combination of three primary color phosphors—red, green and blue phosphor, with light-emitting diode exhibit many problems such as inter-color absorption and the mixing proportion, which affect the luminous efficiency and color rendition to a large extent. However, single-phase white light phosphor can overcome those problems and this ideal scheme has caused the attention of more and more researchers, which will be the trend of development in the future. Eu^{2+}/Mn^{2+}-codoped single-phase white light systems were a potentially ideal candidate, because Eu^{2+} can produce an intense emission band from blue to green, transition metal Mn^{2+} can give abroad emission band from green to red by energy transfer. For instance, $Ba_3MgSi_2O_8$:Eu^{2+},Mn^{2+} [7], $Sr_3Y(PO_4)_3$:Eu^{2+},Mn^{2+} [8], $SrAl_2B_2O_7$:Eu^{2+},Mn^{2+} [9], Na(Sr, Ba)PO_4:Eu^{2+},Mn^{2+} [10].

Dy^{3+} is one of the important rare-earth ions for the preparation of phosphors and plays a major role in the production of different types of light-emitting materials. Because the 4F state of Dy^{3+} ion is easily affected by the outer crystal field, $^4F_{9/2}-{}^6H_J$ ($J=5/2$, 7/2, 9/2, 11/2, 13/2, 15/2) transitions can be obtained in different substrates. Phosphors doped Dy^{3+} ion can produce mainly blue emission (≈ 480 nm), yellow emission (≈ 575 nm), red emission(≈ 670 nm), corresponding to the $^4F_{9/2}-{}^6H_{15/2}$, $^4F_{9/2}-{}^6H_{13/2}$ and $^4F_{9/2}-{}^6H_{11/2}$ transition of Dy^{3+} ion. For instance, Bandi et al. proposed a novel white phosphor $Ca_3Y_{1.92}Si_3O_{12}$:Dy,Ce consisting of blue emission ($^4F_{9/2}-{}^6H_{15/2}$) and the yellow emission ($^4F_{9/2}-{}^6H_{13/2}$) [11], Lupei et al. [12] investigated spectroscopic characteristics of Dy^{3+}-doped $Y_3Al_5O_{12}$, peaking at 485 nm ($^4F_{9/2}-{}^6H_{15/2}$), 580 nm ($^4F_{9/2}-{}^6H_{13/2}$), and 675 nm ($^4F_{9/2}-{}^6H_{11/2}$) [12].

---

*Corresponding author. Tel.: +86 13 842 060 909.
E-mail address: cyj200507@yahoo.com.cn (Y.-J. Chen).

0272-8842/$ - see front matter © 2012 Elsevier Ltd and Techna Group S.r.l. All rights reserved.
http://dx.doi.org/10.1016/j.ceramint.2012.09.038

The T phase of $Ba_{1.3}Ca_{0.7}SiO_4$ host lattice is the most chemically stable one in $(Ba,Ca)_2SiO_4$ system [13]. White-light phosphor has been obtained when Eu^{2+} and Mn^{2+} were doped simultaneously in this T-phase substance [14]. In this paper, we report the synthesis and characteristics of a series of T phase full-color emitting $Ba_{1.3}Ca_{0.69-x-y}SiO_4$ (BCS):$0.01Eu^{2+}$,xMn^{2+}, yDy^{3+} phosphors, and photoluminescence (PL) and the photochromic parameters of the phosphors are determined. By tuning the Mn^{2+} content, white light phosphors with different color rendering indexes and color temperatures have been synthesized.

2. Experimental procedure

A solid-state synthesis procedure was used to prepare the phosphors with nominal compositions of $Ba_{1.3}Ca_{0.69-x-y}SiO_4$:$0.01Eu^{2+}$,$xMn^{2+}$,$yDy^{3+}$(BCS–EMD). Ca^{2+} was substituted by Mn^{2+} and Dy^{3+}. The starting materials were $CaCO_3$ (A.R. grade), $BaCO_3$ (A.R. grade), SiO_2 (A.R. grade), $MnCO_3$ (A.R. grade), Eu_2O_3 (99.99% purity), Dy_2O_3 (99.99% purity). 7 mol % of $BaCl_2 2H_2O$ (A.R. grade) was added additionally as a fluxing agent. All raw materials with stoichiometric amounts were mixed thoroughly with amounts of ethanol in an agate mortar. Then these mixtures were dried at 50 °C for 1 h. Finally, the obtained powder was reground and calcined in a tubular furnace at 1000 °C for 2 h in a reductive atmosphere (the composition of mixed flowing gas is $V_{(H2)}/V_{(N2)}=1/10$). The sample was allowed to cool spontaneously in the reducing atmosphere to 400 °C, then kept on cooling to room temperature spontaneously in air atmosphere. Accordingly, the reaction equation can be expressed as follows:

$$1.3BaCO_3+(0.69-x-y)CaCO_3+0.005Eu_2O_3 \\ +xMnCO_3+y/2Dy_2O_3+SiO_2\rightarrow \\ Ba_{1.3}Ca_{0.69-x-y}SiO_4{:}0.01Eu,xMn,yDy+(1.99-y)CO_2\uparrow; \\ x,\ y=0\text{–}0.05$$

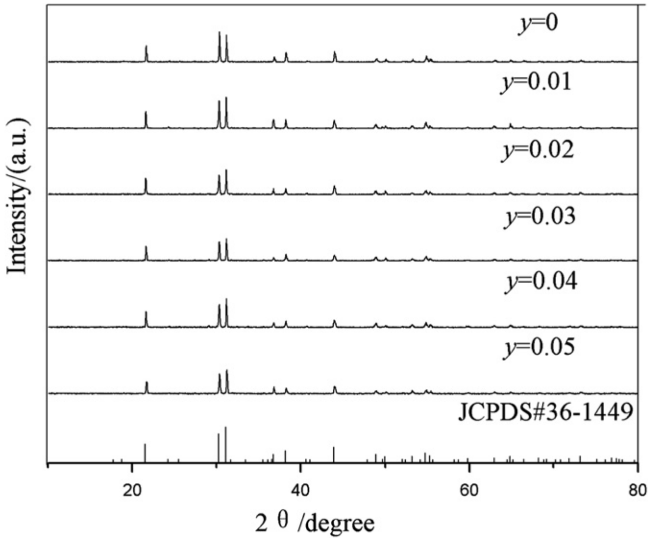

Fig. 1. The XRD patterns of BCS:$0.01Eu^{2+}$,$0.02Mn^{2+}$,yDy^{3+} ($y=0$–0.05) phosphors.

The structure of the products was characterized by the XRD employing Cu K_α radiation at 40 kV and 250 mA, the diffraction data were recorded over the range $\theta=10$–80° with a 0.02° step size, a scan speed of 4 °/min. The PL and PL excitation (PLE) spectra of the samples were recorded with Hitachi F-4600 fluorescence spectrophotometer equipped with a 150 W Xenon lamp under a working voltage of 500 V. Thermoluminescence spectra were recorded using the RGD3B thermoluminescence dosimeter (Beijing Institute of Chemical Defense), heating rate 8 °C/s, maintaining 40 °C for 8 s and 300 °C for 12 s. The sample weight was kept constant (0.0007 g). The photochromic parameters of phosphors were measured with a PMS-50 (PLUS) UV–vis–near IR spectrophotocolorimeter, scan rate 5 nm/s, excitation wave-length 365 nm. All these measurements were carried out at room temperature.

3. Results and discussion

The XRD patterns of BCS:$0.01Eu^{2+}$,xMn^{2+},yDy^{3+} ($y=0$–0.05 mol%) samples are shown in Fig. 1. All diffraction peaks of these samples coincide well with the Joint Committee on Powder Diffraction Standards (JCPDS) card No. 36-1449, no obvious shifting of peaks or other impurity phase can be detected at the current doping level. From Rietveld refinement of the JADE 5.0 software package, the calculated lattice parameters are shown in Table 1. Compared with the standard crystal (T phase), the value of a, c, V has scarcely changed, which

Table 1
Unit cell parameters of BCS:$0.01Eu^{2+}$,$0.02Mn^{2+}$,yDy^{3+} ($y=0$–0.05) phosphors.

y	a (Å)	c (Å)	V (Å^3)	Z	Density
0	5.739	14.634	417.38	4.0	4.7684
0.01	5.741	14.656	418.40	4.0	4.7569
0.02	5.746	14.664	419.29	4.0	4.7467
0.03	5.741	14.647	418.14	4.0	4.7598
0.04	5.742	14.651	418.31	4.0	4.7579
0.05	5.739	14.645	417.72	4.0	4.7645
Standard crystal	5.749	14.664	419.73	4.0	4.7418

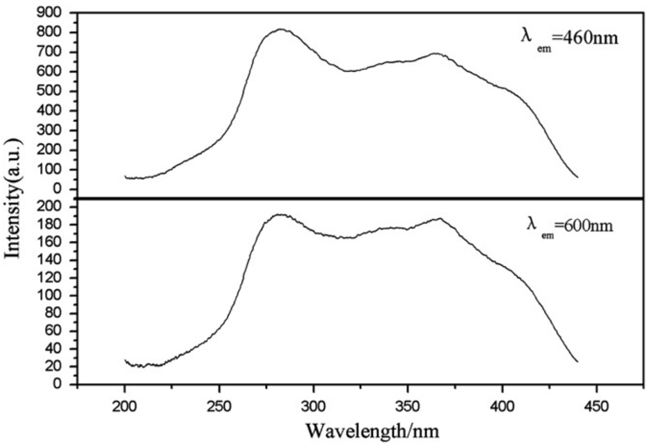

Fig. 2. PLE spectra of BCS:0.01Eu^{2+},0.02Mn^{2+},0.02Dy^{3+} monitored under 460 nm and 600 nm.

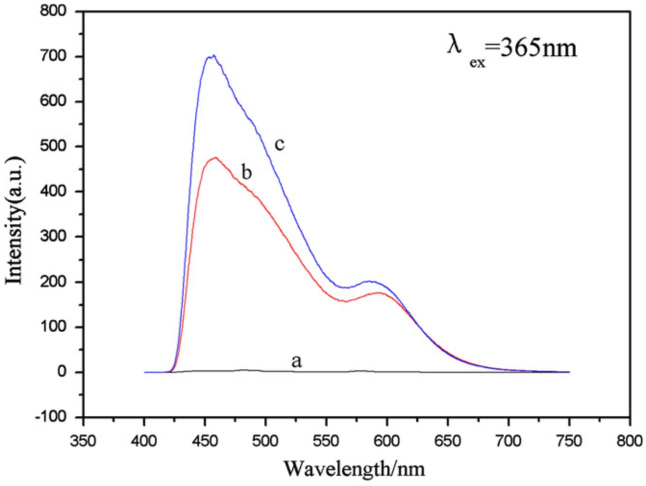

Fig. 3. PL spectra ($\lambda_{ex}=365$ nm) of (a) BCS:0.02Dy^{3+}; (b) BCS:0.01Eu^{2+},0.02Mn^{2+}; and (c) BCS: 0.01Eu^{2+},0.02Mn^{2+},0.02Dy^{3+}.

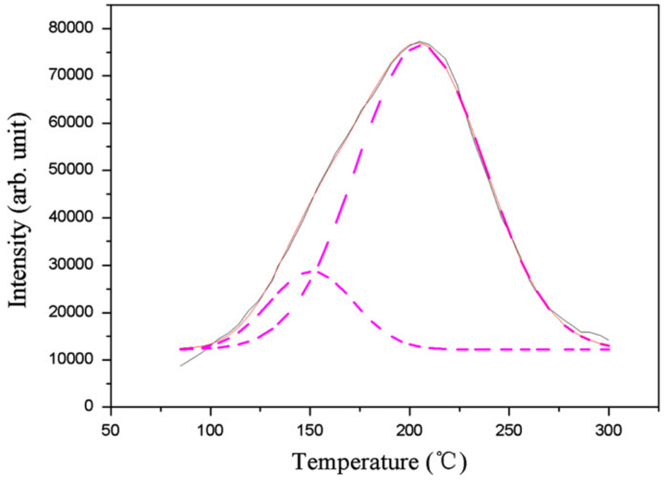

Fig. 4. The TL curve of BCS:0.01Eu^{2+},0.02Mn^{2+},0.02Dy^{3+} phosphor and two sub-bands fitted by Gaussian function.

indicates that Ca^{2+} can be partly replaced by rare-earth ions (Eu^{2+}, Dy^{3+}) and Mn^{2+} ions without change of crystal structure. The standard crystal belongs to the P3m1 space group with hexagonal unit cell ($a=5.749$ Å, $c=14.664$ Å, $V=419.73$ Å^3 for Ba$_{1.3}$Ca$_{0.7}$SiO$_4$). It consists of five Ba^{2+}/Ca^{2+} sites (one M(2)O$_6$ ring and four M(1, 3, 4, 5)O$_{10/12}$ polyhedrons) and two SiO$_4$ tetrahedral sites [15].

The PLE spectra of BCS:0.01Eu^{2+},0.02Mn^{2+},0.02Dy^{3+} sample monitored under 460 nm and 600 nm monitored are given in Fig. 2. The two PLE spectra monitored under 460 nm (main emission peak of Eu^{2+}) and 600 nm (emission peak of Mn^{2+}) are similar and exhibit a wide band extending from 230 to 440 nm, which contain mainly two absorption bands peaking at about 283 and 365 nm. The BCS–EMD sample has the larger energy absorption at 283 nm than at 365 nm UV radiation, but it is cheap and available commercially for LED-chip with 350–410 nm, the wavelength of 365 nm was chosen as excitation wavelength in this paper.

The PL spectra of BCS:0.02Dy^{3+}, BCS:0.01Eu^{2+},0.02 Mn^{2+} and BCS:0.01Eu^{2+},0.02Mn^{2+}, 0.02Dy^{3+} phosphors excited at 365 nm are given clearly in Fig. 3. There are rarely emission peak in the PL spectra of BCS:0.02Dy^{3+} phosphor, which demonstrates that Dy^{3+} cannot be used as the luminescent center in the BCS host crystal lattice. However, the intensity of PL spectrum enhances clearly with the incorporation of Dy^{3+} in BCS:Eu^{2+},Mn^{2+}crystal lattice. The BCS:Eu^{2+},Mn^{2+} phosphor has been observed and discussed by Park et al. [16], the energy transfer between Eu^{2+}–Mn^{2+} was induced by dipole-quadrupole interaction. The characteristic emission peaks (any sharp 4F–6H transitions) of Dy^{3+} are not present in BCS:Eu^{2+},Mn^{2+},Dy^{3+} crystal lattice, which indicates that Dy^{3+} might act as a sensitizer and transfer energy to Eu^{2+} with the function of the hole and electron traps [17].

Fig. 4 plots the TL glow curve of the BCS:0.01Eu^{2+}, 0.02Mn^{2+},0.02Dy^{3+} phosphor. The TL curve is intensive, which indicates that more electrons can be trapped by co-doping Dy^{3+} ions. Here Gaussian fitting was done for resolving the TL curve, revealing two obvious peaks at 151 °C and 206 °C, demonstrating the existence of two traps in the material. The activation energy of the traps was calculated using the following equation [18],

$$E=2KT_m^2/T_2-T_1$$

where K is Boltzmann constant, T_m is the temperature at the peak maximum and (T_2-T_1) is the width of half-maximum of the peak. The corresponding data of the TL peaks are listed in Table 2. The activation energy data of 0.43 eV and 0.45 eV show they are the shallow trap defects, and these trap defects could easily release electrons. It further demonstrates the energy transfer mechanism of Dy–Eu through the process of hole and electron traps.

The schematic graph of energy transfer mechanism of Dy–Eu in BCS–EMD phosphor is represented in Fig. 5.

Table 2
The TL date of the BCS:$0.01Eu^{2+}$,$0.02Mn^{2+}$,$0.02Dy^{3+}$ sample.

Peak	T_m/°C	T_1/°C	T_2/°C	E/ev
a	151	123	195	0.43
b	206	162	251	0.45

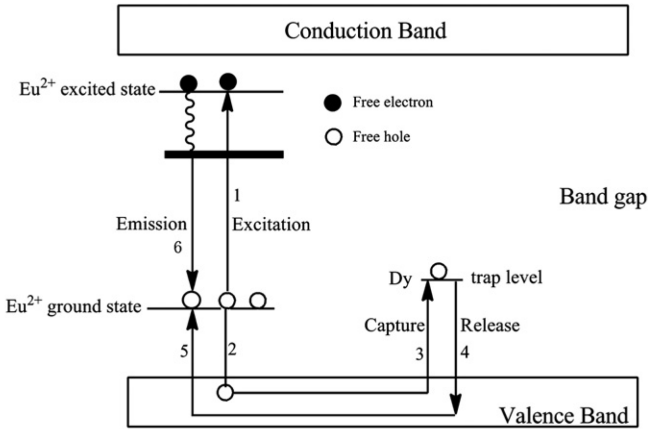

Fig. 5. The schematic graph of energy transfer mechanism of Dy–Eu in BCS–EMD phosphor.

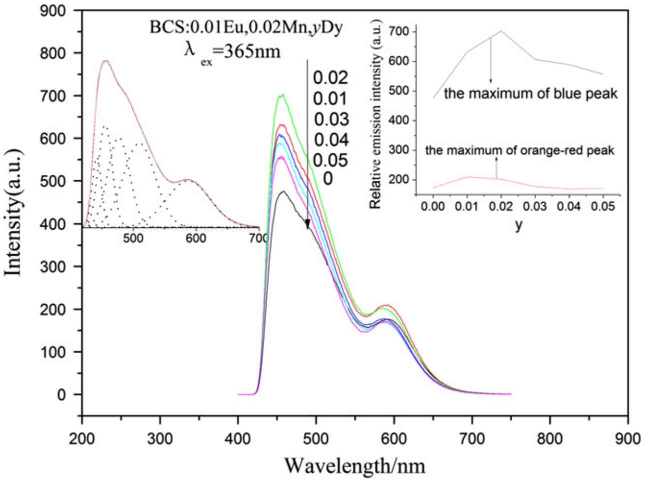

Fig. 6. PL spectra (λ_{ex}=365 nm) of BCS:$0.01Eu^{2+}$,$0.02Mn^{2+}$,yDy^{3+} with different Dy^{3+} concentrations, the left insets show five sub-bands fitted by Gaussian function (dotted lines) with $x=y=0.02$, the right insets show the maximum of blue emission band and orange-red emission band with different y value.

Under the UV excitation, the electrons absorbed energy of ground state ($4f^7$) of Eu^{2+} are excited to the excited state ($4f^65d^1$), generating some holes simultaneously (process 1). Part of the holes are released to valence band (process 2), and captured by co-doping Dy^{3+} ion (process 3), energy of holes is stored temporarily in the crystal, forming metastable state. After heated, stored holes are released to valence band (process 4), migrate to ground state (process 5), then recombine with free electrons from excited state (process 6). The combination of stimulated holes and free electrons radiates spontaneously visible light, which improves the luminescence intensity.

The PL spectra of BCS:$0.01Eu^{2+}$,$0.02Mn^{2+}$,yDy^{3+} samples exhibit a broad nonsymmetrical band in the wavelength range of 420–563 nm with two peaks centered at about 455 nm and 496 nm, as shown in Fig. 6. They are fitted by Gaussian function and then form four sub-bands peaking at about 442 nm, 456 nm, 477 nm, 511 nm (dotted lines), as shown by the left inset in Fig. 6. This is due to the substitution of four possible M(1, 3, 4, 5)$O_{10/12}$ sites or partial M(2)O_6 sites by Eu^{2+} ions. A weak broad band from 563 to 670 nm centered at 591 nm occurs in Eu/Mn and Eu/Mn/Dy phosphors, which can be assigned to $^4T_1(^4G)\rightarrow{}^6A_1(^6S)$ forbidden transition of Mn^{2+}. From Fig. 6, we can also see that the PL intensity enhances gradually with the increase of y value from 0 to 2 mol%. When Dy^{3+} concentration is 2 mol%, the luminescence intensity at 455 nm reaches the optimum, luminescence intensity centered at 455 nm and 596 nm is 147% and 115% as that of un-doped sample, respectively, as shown in the right inset of Fig. 6. The intensity falls gradually when Dy^{3+} dopant is higher above 2 mol%. One of the possible explanations for this luminescence decay is Dy^{3+} concentration quenching, which occurred frequently in rare earth ions doped materials as the ions concentration is over-saturation [19]. Another reason may be closely related to chemical clustering that increases ion–ion interaction of Dy^{3+}, reduces the number of Dy^{3+} ions, which is truly involved in energy transfer process. Thus, the fewer holes and traps were generated in this system, which weakens the energy transfer of Dy–Eu [20]. The CIE chromaticity coordinates, CCT and CRI of BCS:$0.01Eu^{2+}$, $0.02Mn^{2+}$, yDy^{3+} phosphors with different doping contents of Dy^{3+} excited at 365 nm are summarized in Table 3. As the value of y increases from 0 to 5 mol%, the CIE chromaticity coordinates of the phosphors all fall in the white region, as represented in points F to K in Fig. 7. The findings showed that the luminescence intensity of BCS–EMD phosphors can be improved obviously via adding Dy^{3+}, but less influence to light-color parameter.

The PL spectra of BCS:$0.01Eu^{2+}$,xMn^{2+},$0.01Dy^{3+}$ phosphors with different Mn^{2+} concentration are shown in Fig. 8. It is clearly observed that no obvious orange-red light occurs in spectrum when x value is 1 mol%, because of the insufficient Mn^{2+} content and lack of energy transfer between Eu^{2+} and Mn^{2+}. With the increase of x value, the intensity of the orange-red emission band increases, when x is 3 mol%, it reaches maximum. Whereas the intensity of the blue emission band decreases simultaneously. These results indicate that the energy transfer occurs from Eu^{2+} to Mn^{2+}.

With Mn^{2+} dopant concentration higher than 3 mol%, the emission intensity of the whole spectra begins to decrease because of the exceeding Mn^{2+} killing the luminous centers

Table 3
Comparison of CIE chromaticity coordinates (x, y), CCT (T_c) and CRI (R_a) for BCS:0.01Eu^{2+},0.02Mn^{2+},$y$$Dy^{3+}$ phosphors excited at 365 nm.

Sample no.	Sample composition (y)	CIE coordinates (x, y)	CCT (T_c/K)	CRI (R_a/%)
F	0	0.3246, 0.3161	5917	83.5
G	0.01	0.3119, 0.3036	6804	82.7
H	0.02	0.2941, 0.2937	8416	84.3
I	0.03	0.2964, 0.2949	8172	84.1
J	0.04	0.2936, 0.2890	8628	83.7
K	0.05	0.3023, 0.2917	7748	82.1

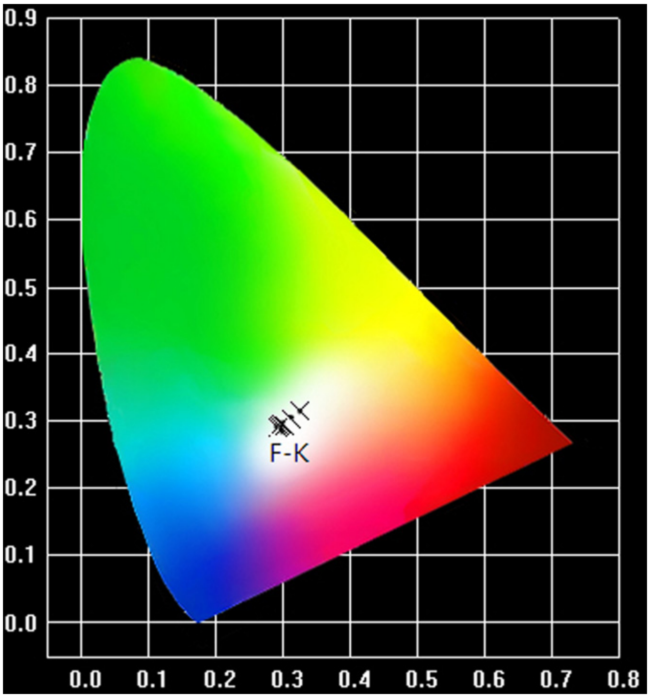

Fig. 7. CIE chromaticity diagram for BCS:0.01Eu^{2+},0.02Mn^{2+},$y$$Dy^{3+}$ phosphors (point F–K) excited at 365 nm.

and concentration quenching among Mn^{2+} ions. Similar phenomenon was observed and discussed by Ruelle et al. [21]. The possible reason is attributed to the paired Mn^{2+} centers decaying faster than single Mn^{2+} centers. The CIE chromaticity coordinates, CCT and CRI of BCS:0.01Eu^{2+}, $x$$Mn^{2+}$,0.01$Dy^{3+}$ phosphors with different doping contents of Mn^{2+} excited at 365 nm are summarized in Table 4. As x increases from 1 to 5 mol%, the values of R_a and T_c decrease gradually, the CIE chromaticity coordinates of the phosphors is tuned from blue to orange-red clearly, as represented in points A to E in Fig. 9, which demonstrates that the luminescent characteristics of the phosphors can be regulated. In particular, a white light phosphor (BCS:0.01Eu^{2+}, 0.02Mn^{2+},0.02Dy^{3+}) with CIE chromaticity coordinates of (0.2941, 0.2937), CCT of T_c = 8416 K, an excellent CRI of R_a=84.3% (higher than that R_a ($\approx$78) of a W-LED based on commercial YAG:Ce pumped by blue InGaN chip) can be obtained by regulating the Mn^{2+} content in the single host.

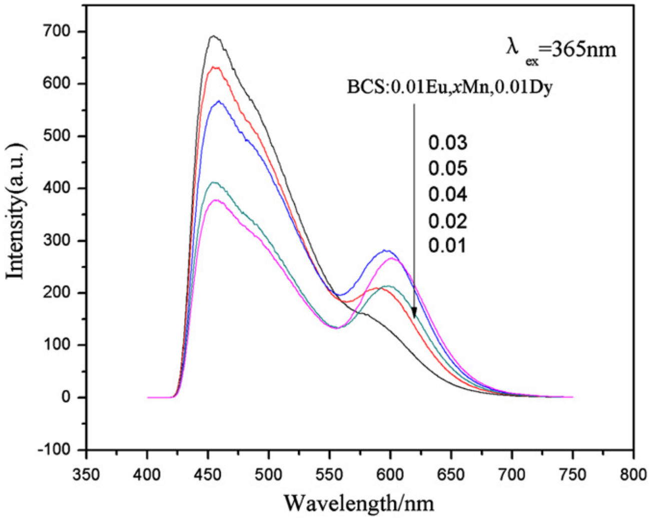

Fig. 8. PL spectra (λ_{ex}=365 nm) of BCS:0.01Eu^{2+},$x$$Mn^{2+}$,0.01$Dy^{3+}$ with different Mn^{2+} concentrations.

Table 4
Comparison of CIE chromaticity coordinates (x, y), CCT (T_c) and CRI (R_a) for BCS:0.01Eu^{2+},$x$$Mn^{2+}$,0.01$Dy^{3+}$ phosphors excited at 365 nm.

Sample no.	Sample composition (x)	CIE coordinates (x, y)	CCT (T_c/K)	CRI (R_a/%)
A	0.01	0.2631, 0.2898	12084	86.5
B	0.02	0.3119, 0.3036	6804	82.7
C	0.03	0.3589, 0.3247	4292	78.4
D	0.04	0.3662, 0.3171	3922	75.4
E	0.05	0.4015, 0.3276	2961	71.3

4. Conclusions

A series of BCS–EMD phosphors with varying Mn^{2+}/Dy^{3+} were prepared successfully by the solid state reaction method. The emission spectra of these phosphors showed that the two main peaks are located at 455 and 596 nm, which can be assigned to 5d→4f transition of Eu^{2+}, and $^4T_1(^4G)\rightarrow{}^6A_1(^6S)$ forbidden transition of Mn^{2+}, respectively. Dy^{3+} enhances clearly the luminescence intensity of BCS:Eu^{2+},Mn^{2+} phosphors. Dy^{3+} ions might act as sensitizer. It is probable that energy transfer from Dy^{3+} to Eu^{2+} occurs through the function of hole and electron traps. Color-tunable white light phosphors can be obtained via changing the Mn^{2+} content. A outstanding phosphor (BCS:0.01Eu^{2+},0.02Mn^{2+},0.02Dy^{3+}) with CIE chromaticity coordinates of (0.2941, 0.2937), an excellent CRI of R_a=84.3%, and CCT of T_c=8416 K was obtained. In addition, these phosphors could be efficiently excited in the wavelength range of 350–410 nm where the near ultraviolet light-emitting diode is well matched. According to these excellent spectra profile, we could conclude that the BCS–EMD phosphor might be a promising single-phased phosphor for near-UV white-light LED.

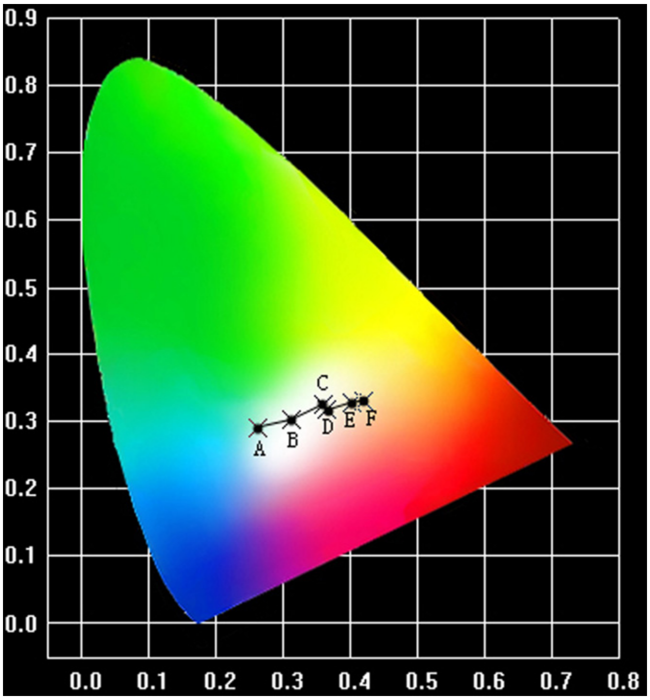

Fig. 9. CIE chromaticity diagram for BCS:0.01Eu^{2+},xMn^{2+},0.01Dy^{3+} phosphors (point A–E) excited at 365 nm.

Acknowledgments

The authors are grateful for the Science and Technical Project of Liaoning Province of PR China (Grant no. LS 2010120), and the Natural Science Project of Liaoning Province of PR China (Grant no. 201102174).

References

[1] T. Jüstel, H. Nikol, C. Ronda, New developments in the field of luminescent materials for lighting and displays, Angewandte Chemie-International Edition 37 (1998) 3084–3103.

[2] Y.C. Xu, D.H. Chen, Combustion synthesis and photoluminescence of $Sr_2MgSi_2O_7$:Eu,Dy long lasting phosphor nanoparticles, Ceramics International 34 (2008) 2117–2120.

[3] F.B. Cao, Y.W. Tian, Y.J. Chen, L.J. Xiao, Y.Y. Liu, L.K. Li, Preparation and luminescent properties of novel red phosphors for white-light emitting diodes (W-LEDs) application, Materials Science in Semiconductor Processing 12 (2009) 94–98.

[4] Y.J. Lu, G.Y. Shi, Q.H. Zhang, H.Z. Wang, Y.G. Li, Photoluminescence properties of Eu^{2+} and Mg^{2+} co-doped $CaSi_2O_2N_2$ phosphor for white light LEDs, Ceramics International 38 (2012) 3427–3433.

[5] H.S. Roh, I.S. Cho, J.S. An, C.M. Cho, T.H. Noh, D.K. Yim, D.W. Kim, K.S. Hong, Enhanced photoluminescence property of Dy^{3+} co-doped $BaAl_2O_4$:Eu^{2+} green phosphors, Ceramics International 38 (2012) 443–447.

[6] Y.J. Chen, Z. Huang, L.K. Li, X.J. Geng, T.T. Liu, Y. Xie, L.J. Xiao, Synthesis and luminescent properties of single-phase white light-emitting $Ba_{1.3}Ca_{0.7}SiO_4$ phosphors, Journal of the Chinese Ceramic Society 39 (2011) 1406–1410.

[7] J.S. Kim, P.E. Jeon, J.C. Choi, H.L. Park, Warm-white-light emitting diode utilizing a single-phase full-color $Ba_3MgSi_2O_8$:Eu^{2+},Mn^{2+} phosphor, Applied Physics Letters 84 (2004) 2931–2933.

[8] N. Guo, Y.J. Huang, M. Yang, Y.H. Song, Y.H. Zheng, H.P. You, A tunable single-component warm white-light $Sr_3Y(PO_4)_3$:Eu^{2+}, Mn^{2+} phosphor for white-light emitting diodes, Physical Chemistry Chemical Physics 13 (2011) 15077–15082.

[9] L.Y. Zhou, L.H. Yi, X.M. Feng, New $SrAl_2B_2O_7$:Eu^{2+}, Mn^{2+} phosphors for white light-emitting diodes, Spectrochimica Acta A 83 (2011) 340–343.

[10] S.H. Choi, Y.J. Yun, H.K. Jung, Eu^{2+} and Mn^{2+} activated single phase white emitting phosphor Na(Sr,Ba)PO_4 for phosphor converted-LEDs, Materials Letters 75 (2012) 186–188.

[11] V.R. Bandi, Y.T. Nien, T.H. Lu, I.G. Chen, Enhancement of white light emission from novel $Ca_3Y_2Si_3O_{12}$:Dy^{3+} phosphors with Ce^{3+} ion codoping, Journal of Applied Physics 108 (2010) 23111–23115.

[12] A. Lupei, V. Lupei, C. Gheorghe, A. Ikesue, M. Enculescu, Spectroscopic characteristics of Dy^{3+} doped $Y_3Al_5O_{12}$ transparent ceramics, Journal of Applied Physics 110 (2011) 083120.

[13] B. Matković, S. Popović, B. Gržeta, Phases in the System Ba_2SiO_4–Ca_2SiO_4, Journal of the American Ceramic Society 69 (1986) 132–134.

[14] N.S. Choi, K.W. Park, B.W. Park, X.M. Zhang, J.S. Kim, P. Kung, S.M. Kim, Eu^{2+}–Mn^{2+} energy transfer in white-light-emitting T-phase $(Ba,Ca)_2SiO_4$:Eu^{2+},Mn^{2+} phosphor, Journal of Luminescence 130 (2010) 560–566.

[15] A.Koichiro Fukuda, Masamichi Ito, Tomoyuki Iwata, Crystal structure and structural disorder of $(Ba_{0.65}Ca_{0.35})_2SiO_4$, Journal of Solid State Chemistry 180 (2007) 2305–2309.

[16] K. Park, N.S. Choi, J.S. Kim, P. Kung, S.M. Kim, Temperature and excitation power-resistant white-light emission of theT-phase $(Ba,Ca)_2SiO_4$:Eu^{2+},Mn^{2+} phosphor, Solid State Communications 150 (2010) 329–332.

[17] A.A.S. Alvani, F. Moztarzadeh, A.A. Sarabi, Effects of dopant concentrations on phosphorescence properties of Eu/Dy-doped $Sr_3MgSi_2O_8$, Journal of Luminescence 114 (2005) 131–136.

[18] Meril Mathew, Engineering the Properties of Indium Sulfide for Thin Film Solar Cells by Doping, Cochin University, India, 2009, p. 126.

[19] F. Zhang, Z.S. Xiao, F. Zhu, L. Yan, B. Zhou, A.P. Huang, Photoluminescence and energy transfer study of Er^{3+} and Dy^{3+} codoped tellurite glasses, Journal of Nanoscience and Nanotechnology 11 (2011) 10904–10907.

[20] F. Auzel, P. Goldner, Towards rare-earth clustering control in doped glasses, Optical Materials 16 (2001) 93–103.

[21] N. Ruelle, M.P. Thi, C. Fouassier, Cathodoluminescent properties and energy transfer in red calcium sulfide phosphors (CaS:Eu,Mn), Japanese Journal of Applied Physics 31 (Pt 1,9A) (1992) 2786–2790.